

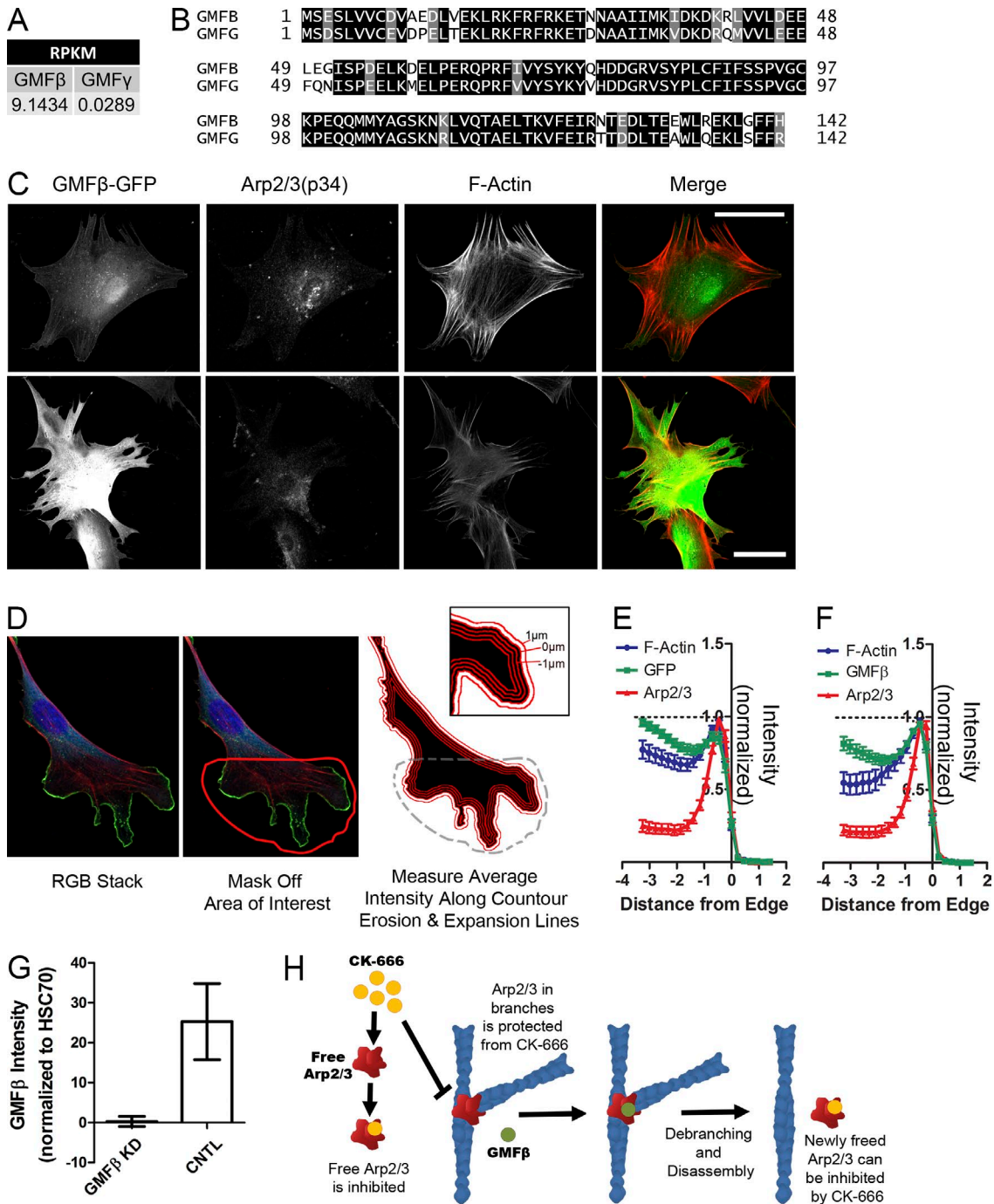
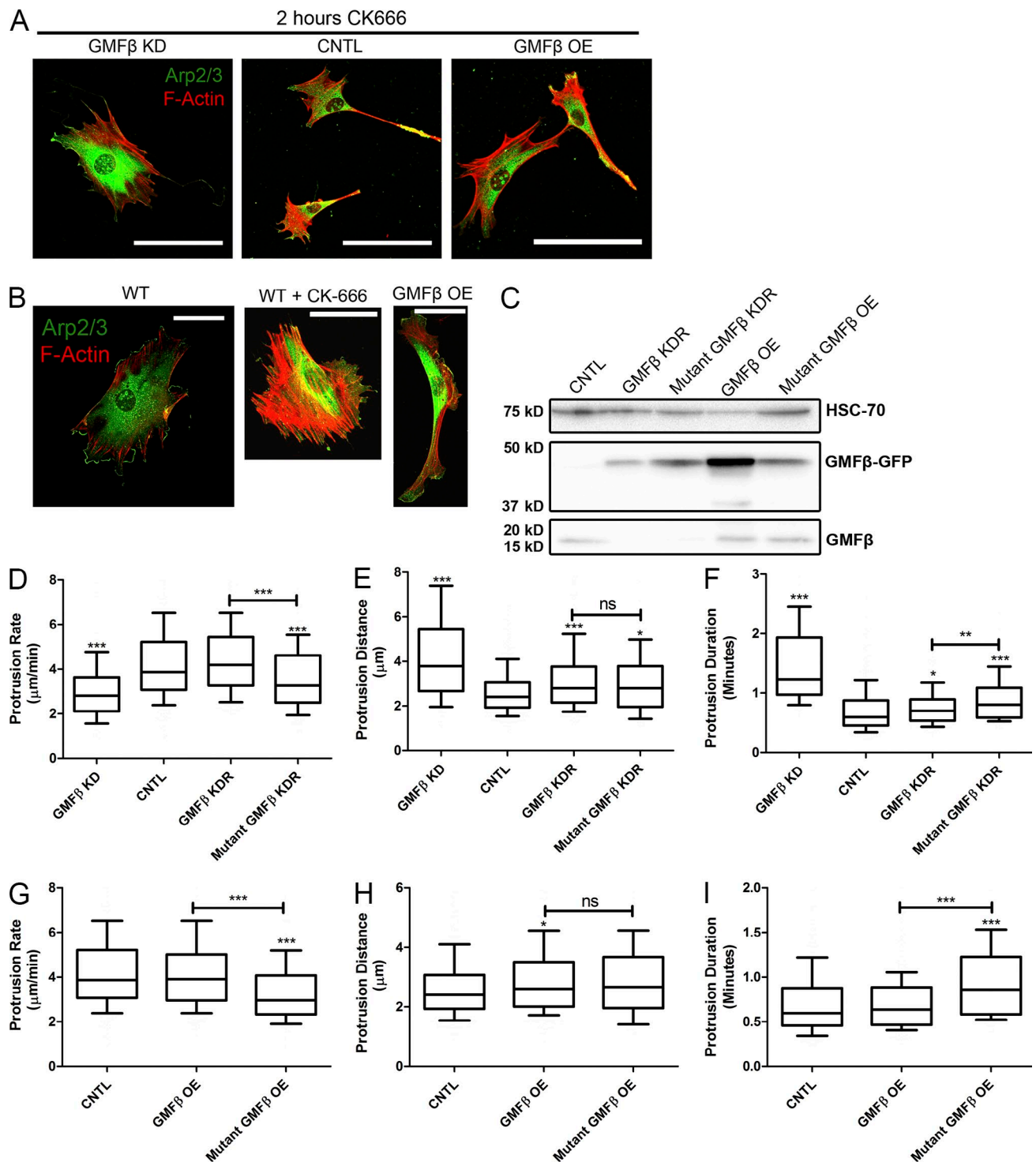
Haynes et al., <http://www.jcb.org/cgi/content/full/jcb.201501094/DC1>

Figure S1. **GMFβ but not GMFγ is expressed in fibroblasts and localizes specifically to the leading edge.** CK-666, a small molecular inhibitor of Arp2/3, can be used to provide insights on Arp2/3. This figure is related to Figs. 1 and 3. (A) GMFβ versus GMFγ expression in our mouse embryonic fibroblast line as measured by RNA-seq analysis. RPKM = reads per kilobase of transcript per million mapped reads. (B) Sequence alignment of human GMFβ (GMFB) with human GMFγ (GMFG). (C) Cells depleted of two subunits of Arp2/3 (p34Arc and Arp2) have no lamellipodia and do not display GMFβ-GFP localization at the cell edge. Bars, 50 μm. (D) Example of contour erosion line scans (right) generated from a fluorescent image of a cell (left). The edge of the cell is detected using an ImageJ macro, and line scans for a user-defined area of the cells (such as the lamellipodia) are generated automatically at various distances from the cell edge. Here, example contour lines are drawn at 1-μm intervals. The average fluorescence intensity for the lines inside the defined region is recorded and plotted. (E) Edge intensity map generated for GFP-expressing cells. Fluorescence for each channel is normalized to the highest intensity value for that channel in the entire cell. GFP reaches peak fluorescence intensity toward the inside of the cell, away from the leading edge marker Arp2/3. (F) Edge intensity map generated for GMFβ-GFP-expressing cells. GMFβ-GFP reaches peak fluorescence intensity at the cell edge, comparable to Arp2/3. (G) Quantification of GMFβ knockdown via Western blotting of lysates from four separate experiments. GMFβ intensity and HSC70 (control) intensity was measured with local background subtracted, then the GMFβ signal was divided by the HSC70 signal to normalize. Error bars indicate the 95% confidence interval. (H) The CK-666 wash-in experiment: when 150 μM CK-666 is added to cells, Arp2/3 that is not occupied in branches is bound by CK-666 and inactivated, preventing new branch formation. Arp2/3 that is currently in branches is protected from CK-666 until it is turned over by debranching or disassembly (for example, by GMFβ). Once Arp2/3 is removed from the branch and becomes free again, CK-666 can bind it and block its incorporation into new branches. Therefore, using this assay, the disappearance of Arp2/3 from the leading edge should reflect the disassembly rate of the branch network without any confounding effects of branch creation.



**Figure S2. A debranching-deficient mutant of GMFβ cannot replicate GMFβ overexpression phenotypes or rescue GMFβ depletion.** This figure is related to Fig. 4. (A) Immunostaining of Arp2/3 (anti-p34; green) and F-actin (red) in cells treated with CK-666 for 2 h. Bars, 100 μm. (B) Immunostaining of Arp2/3 (anti-p34) and F-actin in WT cells with synchronized lamellipodia (left), cells treated with CK-666 for 10 min (center), and a GMFβ-overexpressing cell with synchronized lamellipodia (right). CK-666, which inhibits Arp2/3, creates a very distinct phenotype to that of overexpression of GMFβ. Bars, 50 μm. (C) Western blot representing the expression level of mutant GMFβ-GFP compared with WT GMFβ-GFP for various cell types. Expression of mutant GMFβ-GFP to the same levels at WT GMFβ-GFP OE made cells unhealthy and stalled their growth, so a moderate overexpression level was used. (D) Protrusion rate in micrometers per minute for GMFβ-depleted cells rescued with mutant GMFβ-GFP, as quantified from kymography analysis. (E) Protrusion distance in micrometers of GMFβ-depleted cells rescued with mutant GMFβ-GFP, as quantified from kymography analysis. (F) Protrusion duration in minutes of GMFβ-depleted cells rescued with mutant GMFβ-GFP, as quantified from kymography analysis. (G) Protrusion rate in micrometers per minute for mutant GMFβ-overexpressing cells, as quantified from kymography analysis. (H) Protrusion distance in micrometers for mutant GMFβ-overexpressing cells, as quantified from kymography analysis. (I) Protrusion duration in minutes for mutant GMFβ-overexpressing cells, as quantified from kymography analysis. For all graphs, error bars represent the 10th–90th percentile. Kruskal-Wallis multiple comparison testing was performed, and significance was measured with a Dunn's post-test. \*\*\*,  $P < 0.001$ ; \*\*,  $P < 0.01$ ; \*,  $P < 0.05$ .

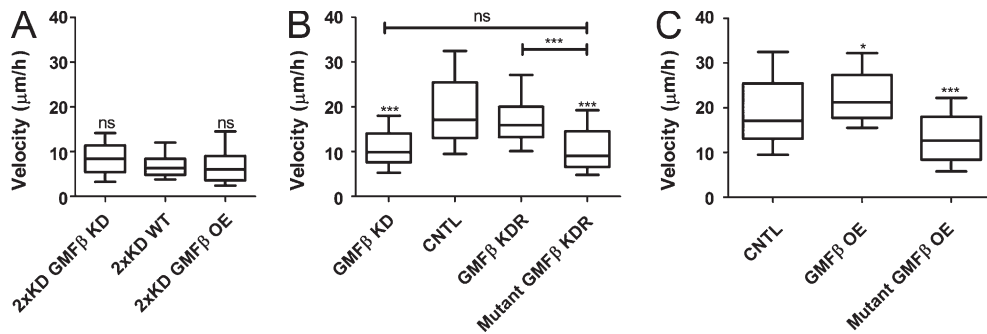
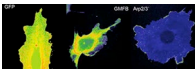
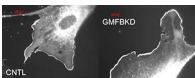


Figure S3. **Cell velocity in cells depleted of Arp2/3 and mutant GMF $\beta$ -expressing cells.** This figure is related to Fig. 5. (A) Single cell velocity was measured for randomly migrating cells depleted of two subunits of Arp2/3 (2xKD). GMF $\beta$  overexpression or depletion had no significant effect on cell velocity in the absence of Arp2/3. KD  $n = 43$ , WT  $n = 42$ , OE  $n = 52$ . (B) Single cell velocity of cells depleted of WT GMF $\beta$  and rescued with mutant GMF $\beta$  randomly migrating. GMF $\beta$  KD  $n = 70$ , CNTL  $n = 64$ , GMF $\beta$  KDR  $n = 77$ , mutant GMF $\beta$  KDR  $n = 98$ . (C) Single cell velocity of mutant GMF $\beta$ -overexpressing cells randomly migrating. CNTL  $n = 70$ , GMF $\beta$  OE  $n = 74$ , mutant GMF $\beta$  OE  $n = 95$ . For all graphs, error bars represent the 10th–90th percentile. Kruskal-Wallis multiple comparison testing was performed, and significance was measured with a Dunn's post-test. \*\*\*,  $P < 0.001$ ; \*\*,  $P < 0.01$ ; \*,  $P < 0.05$ .

Video 1. **Ratiometric movies of GFP, GMF $\beta$ -GFP, and p34-GFP demonstrating that GMF $\beta$  has specific leading edge localization.** Soluble GFP (left), GMF $\beta$ -GFP (center), or p34-GFP (Arp2/3, right) were expressed in cells that also expressed soluble tagRFP-t, and the ratio of the GFP channel to the tagRFP-t channel is displayed. The soluble tagRFP-t and GFP have no specific leading edge localization, so any observed increase at the edge of the cell due to an increase in volume or cell ruffling is eliminated upon creation of the ratio image. Arp2/3 is a reliable marker of the leading edge, and so the ratio of Arp2/3:tagRFP-t shows increased signal only at the edge, with no areas of increased localization in the center of the cell. GMF $\beta$ , compared with GFP alone or Arp2/3, has an intermediate leading edge localization and appears very dynamic in protrusions. Images were acquired every 10 s for 20 min on a confocal microscope (5-Live; Carl Zeiss) with an environmental chamber.



Video 2. **Depletion of GMF $\beta$  increases the stability of p34-GFP at the leading edge upon CK-666 wash-in.** Cells depleted of a subunit of Arp2/3 (p34) and rescued with a GFP-tagged version of that subunit (p34KDR) were treated with the Arp2/3 inhibitor CK-666 (indicated by red text). Upon flow-in of CK-666, CNTL cells immediately lost leading edge p34-GFP signal. Cells depleted of GMF $\beta$ , however, had a slower loss of p34-GFP signal from the leading edge. Cells were imaged on a microscope (IX81; Olympus) using a 60 $\times$ , 1.49 NA objective lens and a camera (Orca-ER; Hamamatsu) controlled by MetaMorph. Images were captured at 5-s intervals as drug was applied, and imaging continued for at least 20 min after addition.



**kmeans1 m** is an accessory file to **arp23edge m**, which allows **kmeans** clustering for detecting the outlines of cells. **colormapb mat** is a color map, which assigns colors to pixel intensities generated by the **arp23edge m** program. **EdgeRatio** is an ImageJ macro for analyzing the localization of proteins along the leading edge. **KymoRate** is a Perl script used for analyzing kymography data. **PercentEdge** is a MATLAB script used for analyzing the percentage of the cell perimeter positive for fluorescent signal. All files are available in a single ZIP file.